



www.sciencemag.org/cgi/content/full/science.aac9819/DC1

Supplementary Materials for

Slow adaptation in the face of rapid warming leads to collapse of the Gulf of Maine cod fishery

Andrew J. Pershing,* Michael A. Alexander, Christina M. Hernandez, Lisa A. Kerr,
Arnault Le Bris, Katherine E. Mills, Janet A. Nye, Nicholas R. Record,
Hillary A. Scannell, James D. Scott, Graham D. Sherwood, Andrew C. Thomas

*Corresponding author. E-mail: apershing@gmri.org

Published 29 October 2015 on *Science Express*
DOI: 10.1126/science.aac9819

This PDF file includes:

Materials and Methods

Supplementary Text

Figs. S1 to S6

Tables S1 to S5

References

Materials and Methods

Sea Surface Temperature Analysis

Our study focuses on the sea surface temperature (SST) trend in the Gulf of Maine. We obtained global SST from NOAA's optimally interpolated SST analysis (<http://www.ncdc.noaa.gov/sst/>)(27). We built a daily climatology for every 0.25° pixel in the global data set over the period 1982-2011 and then computed anomalies from these. This data is available on a daily basis starting in September, 1981.

We defined the Gulf of Maine as the region between latitudes 40.375°N and 45.125°N and longitudes 70.875°W and 65.375°W (Fig. S1). We averaged the SST anomalies over the entire region to produce a daily time series. This time series was then processed into quarterly and annual time series. For display in the text, the daily data were smoothed using a 15 d running mean.

We computed the linear trend ($^{\circ}\text{C yr}^{-1}$) in the daily Gulf of Maine SST time series using standard linear regression. We considered the full time period (1982-2013) and the last decade (2004-2013). SST data is strongly autocorrelated, especially at the daily time scale. The significance values reported in the paper were adjusted for autocorrelation using the method of Pyper and Peterman (28). This method uses a characteristic autocorrelation scale to reduce the degrees of freedom. We used a time scale of 182 days (half of a year), at which point the autocorrelation falls below 0.33. For the full time period, the effective degrees of freedom was 64, while the value for the last decade was 15.

Associations between Gulf of Maine SST and atmospheric and oceanic conditions

To explore potential causes of the recent warming in the Gulf of Maine, we correlated the quarterly Gulf of Maine time series with several standard climate indicators: an index of Gulf Stream position (7, 9), the Pacific Decadal Oscillation (10) (<http://research.jisao.washington.edu/pdo/PDO.latest>), the Atlantic Multidecadal Oscillation (11) (<http://www.esrl.noaa.gov/psd/data/timeseries/AMO/>) and the North Atlantic Oscillation (29) (<https://climatedataguide.ucar.edu/climate-data/hurrell-north-atlantic-oscillation-nao-index-station-based>) (Table S1). All indices were available through 2012.

Based on the results of the correlations, we built linear models for Gulf of Maine summer temperatures using combinations of the Gulf Stream Index (GSI), AMO, and PDO. Models were compared using AIC scores. We further tested the models by examining their ability to explain the recent Gulf of Maine patterns. For each model, we refit the model to data from 1982-2003. We then used the index values from 2004-2012 to estimate the Gulf of Maine temperature. The estimated temperatures were then correlated with the actual temperatures.

Temperature time series and climate indicators used in this study are provided in AVHRRtemperaturedata.csv.

Gulf of Maine cod

Atlantic cod (*Gadus morhua*) are distributed throughout the coastal regions of the North Atlantic, and they are a valuable commercial species across their range. For management purposes, the cod population in US waters is divided into two stocks, a southerly component that includes Georges Bank, and a northerly component referred to as the Gulf of Maine stock (Fig. S1 red line). This stock structure smooths over considerable sub-stock diversity, especially in the Gulf of Maine (30-32).

The Gulf of Maine cod stock was assessed in 2014 by (5). This assessment used fishery dependent data (landings, age and size of catch) through 2013 and fishery independent data (abundance, size and age) through spring 2014 and applied the same statistical catch-at-age model developed during the 2011 benchmark assessment (25). This model reconstructs the age structure (abundance of each age class) for the years 1981-2013 assuming a natural mortality scenario. Two natural mortality scenarios were used in the assessment: one with a constant natural mortality of $M=0.2 \text{ yr}^{-1}$, the other with natural mortality increasing linearly from $M=0.2 \text{ yr}^{-1}$ to $M=0.4 \text{ yr}^{-1}$ over the period 1989-2003. The relationships we report are present in the output of both scenarios. For brevity and to remain consistent with current management of this stock, we present the results using only the $M=0.2$ scenario.

Fisheries population dynamics models require a function relating the abundance of adults to the number of new fish entering the population. This function captures not only the production of larvae or juveniles but encapsulates density-dependence at the adult stage (e.g. competition for food to fuel reproduction) or the larvae/juvenile stage (e.g. competition for habitat). Environmental factors like temperature can be included in these models as well.

We fit three functions relating age-1 cod abundance (R) to spawning stock biomass (S), with and without the effect of temperature (T). The three stock-recruit functions represent different hypotheses about how density dependence impacts recruitment. The Ricker function

$$R = aSe^{bS+cT} \quad (\text{Eq. 1})$$

has the strongest density dependence. When b is negative, per-capita recruitment declines exponentially as S increases. The Beverton-Holt function

$$R = aS(1+bS)^{-1}e^{cT} \quad (\text{Eq. 2})$$

has weaker density dependence. In this model, per-capita recruitment declines approximately as $1/S$. The power-law (also known as a Cushing model)

$$R = aS^b e^{cT} \quad (\text{Eq. 3})$$

has the weakest density dependence. In this model, per-capita recruitment declines approximately as S^{b-1} . The Ricker and Beverton-Holt models are the most common in fisheries applications.

We fit each model to the estimated age-1 abundance using the spawning stock biomass and temperature from the previous year. Both (Eq. 1) and (Eq. 3) can be linearized and solved directly. The Beverton-Holt model with the temperature effect must be solved using numerical optimization. For consistency, we fit all three functions by minimizing

$$\| \log(R_{actual}) - \log(R_{pred}) \| \quad (\text{Eq. 4})$$

where R_{actual} is the observed recruitment (age-1 abundance), R_{pred} is the modeled recruitment, and $\|\bullet\|$ is the Euclidean norm (e.g. the sum of squares). We used Matlab's minimization routine "fminsearch" and confirmed that the solutions for (Eq. 1) and (Eq. 3) were the same as the linear models. We fit the models without a temperature effect and with quarterly and annual average sea surface temperatures from the Gulf of Maine cod stock region (Fig. S1, red line). Models were compared using the r^2 value for the correlation between $\log(R_{actual})$ and $\log(R_{pred})$ and their AIC scores. We also evaluated the models out-of-sample skill by fitting the models to data prior to 2004 and then model recruitment for 2004-2013 using the observed temperature and spawning stock biomass.

The stock assessment for Gulf of Maine cod provides an estimate of the abundance, $N_j(t)$, and catch, $C_j(t)$, where t is the year and the subscript j indicates the age class. The goal of our analysis was to evaluate the stability of model assumptions and whether errors in the assessment are related to temperature.

We began by computing the total mortality ($Z_j(t)$) for each age class in each year:

$$\begin{aligned} N_{j+1}(t+1) &= N_j(t) \exp(-Z_j(t)) \\ Z_j(t) &= \log N_j(t) - \log N_{j+1}(t+1) . \end{aligned} \quad (\text{Eq. 5})$$

The total mortality is the sum of natural mortality ($M_j(t)$) and fishing mortality ($F_j(t)$). The fishing mortality can be computed using the catch ($C_j(t)$):

$$F_j(t)/Z_j(t) = C_j(t) / (N_j(t) - N_{j+1}(t+1)) . \quad (\text{Eq. 6})$$

The natural mortality is then the difference between Z_j and F_j . These calculations assume that abundance is estimated without error by the assessment. In reality, these estimates reflect a complex optimization that attempts to fit the observations of the population and the observed catch.

Using the abundance and catch values from the assessment, we solved for $F_j(t)$ in (Eq. 6). We then correlated the time series for each age class with the quarterly and annual temperature anomalies from the stock region. We focused on the period 1993-2013 for this analysis, as several obvious outliers in the mortality estimates occurred before this period.

To estimate the impact of temperature on the cod populations, we built a simple age-structured population dynamics model. The model assumes that the abundance of age class $j+1$ is related to the abundance of age class j by the fishing mortality (F) and natural mortality (M):

$$N_{j+1}(t+1) = N_j(t) \exp(-F-M) \quad (\text{Eq. 7})$$

This equation applies to age 2-8, with age 9 acting as a plus-group. The fishing mortality on age 1-3 fish was set to zero. The spawning stock biomass is computed at each time step by multiplying the abundance of age 4-9+ by their respective weights (from (33)) and summing. The abundance of age-1 fish is taken from (Eq. 2).

The model was used to explore the impact of temperature on steady-state reference points for the fishery. The model was run using a constant temperature and constant fishing mortality until the population reached steady state. This gives the population biomass and the yield that corresponds to that temperature and fishing intensity. For each temperature, we searched for the fishing mortality that maximized the yield. This gives the standard fishery reference points MSY (maximum sustainable yield), F_{msy} (fishing mortality that produces MSY), and SSB_{msy} (biomass at MSY).

The model was also used to develop a dynamic temperature-dependent SSB_{msy} proxy. The proxy was constructed by simulating a population fished at the steady-state F_{msy} (described above) for the temperature in each year. We began by simulating a population fished for 1000 years at the rate corresponding to the 1982 temperature anomaly. We then allowed F_{msy} to vary according to the observed Gulf of Maine temperature. We used the same approach to estimate the carrying capacity of the population by simulating a population that was never fished. Finally, we simulated a population rebuilding from the 2013 biomass level with fishing mortality set to zero or 0.1. This represents the rebuilding potential of this stock.

Our temperature scenarios were constructed based on observed temperatures from the Gulf of Maine and output from the CMIP5 climate model integration using RCP 8.5 (34). For each member of the CMIP5 ensemble, we computed the mean temperature anomaly from the Northeast US Shelf region. These were standardized so that the 1982-2011 mean anomaly was zero and then smoothed using a 20-year moving average. The ensembles were ranked based on their warming rate after 2000. All scenarios began with the summer Gulf of Maine cod region temperature time series through 2013 (Fig. S3). After 2013, the “cool” scenario used the temperature time series from the 10th coolest ensemble. The “warm” scenario used the ensemble mean time series. For the “hot” scenario, we continued the $0.07^\circ \text{ yr}^{-1}$ trend exhibited

by the summer cod-region temperatures over the 1982-2013 period. Although large, this trend is within the 80% confidence interval of the CMIP ensemble.

The cod population information used in this study, including the calculated extra mortality, are contained in the files `codM02.csv`. The Matlab function `getreferencepoints.m` calculates reference points at a given temperature. It relies on the functions `getyield.m` and `runmodelF.m`.

Supplementary Text

Sea Surface Temperature Analysis

To assess the uniqueness of the recent trend in the Gulf of Maine, we began by computing the 2004-2013 trend at every pixel in the global database. The trends have a median of $-0.003^\circ \text{ yr}^{-1}$, a mean of $0.003^\circ \text{ yr}^{-1}$, and a standard deviation of $0.048^\circ \text{ yr}^{-1}$. There are 691,150 pixels in the database, and only 544 pixels had rates higher than the Gulf of Maine's $0.23^\circ \text{ yr}^{-1}$. This means that the Gulf of Maine warmed faster than 99.9% of the global ocean over this period. Weighting each pixel by its area, the area of ocean with rates greater than the Gulf of Maine's is $310,170 \text{ km}^2$ or 0.09% of the total global ocean area of $3.6 \times 10^8 \text{ km}^2$ (Fig. 1C in main text).

The trend histogram in Fig. 1C could be biased towards regions that, like the Gulf of Maine, have high interannual variability. To verify the uniqueness of the trend, we divided the time series at each pixel by its standard deviation and then computed the trend of the normalized temperature anomaly data. The resulting histogram is skewed towards warming values; however, the Gulf of Maine trend still stands out (Fig. S2A). In this view of the ocean, the Gulf of Maine's trend of 0.27 yr^{-1} is still greater than 99.7% of the ocean, exceeded by only a few pixels in the Atlantic and Indian sectors of the Antarctic Circumpolar Current (Fig. S2B)

As with the higher resolution data, we computed the average warming rate of pixels using the ERSST data from the Gulf of Maine region over 2004-2013. This rate is $0.162^\circ \text{ yr}^{-1}$, slightly lower than the higher resolution data. We then computed the warming rate at each of the 2° -by- 2° ocean pixels. The area of ocean warming faster than the Gulf of Maine is $4.49 \times 10^5 \text{ km}^2$ or 0.12% of the global ocean ($3.75 \times 10^8 \text{ km}^2$) (Fig. S3A).

We then computed the warming rates for each pixel for each 10 year period beginning in January 1900 (Fig. S3B). We only considered periods starting in January. Out of a total of $3.93 \times 10^{10} \text{ km}^2$ considered, the total area of ocean that had warming rates faster than the recent rate in the Gulf of Maine was $1.13 \times 10^8 \text{ km}^2$, or only 0.29%. Thus, the current warming rate in the Gulf of Maine is highly unusual, even by historical standards.

Gulf of Maine Cod Recruitment and Temperature

The performance of the three stock-recruit models was largely similar (Table S2). The base models without temperature were significant but explained only 29% of the variance. Adding a temperature effect improved the performance; however, only the models from the third quarter (summer) and annual average temperatures lowered the AIC score by an appreciable amount. The summer models were the best, and these models had considerable out of sample skill.

The differences between the model types were subtle, but consistent. As density dependence weakened, the fit of the summer and annual average temperature models improved, with the power-law models being the best overall. The coefficients for the summer models are provided in Table S3.

Gulf of Maine Cod Mortality and Temperature

We found the strongest correlations between temperature and the mortality correction for the age 4 fish (Table S4), with the relationship with the fall temperatures especially strong ($r=0.68$, $p<0.01$, $n=20$). The age 4 correlations were all positive, indicating extra mortality during warm years. The correlations with summer, fall, and annual mean temperature are all significant, even if the last two years (the two warmest in the time series) are removed.

Age 4-5 fish dominate the biomass of the population and the catch, and changes in the survival of these fish will have a significant impact on the population dynamics of the stock. To further explore the relationship between this critical age class and temperature, we built multiple linear regression models between the age 4 mortality correction and combinations of fall temperatures at several lags (Table S5). The strongest relationships used temperatures from the first and fourth years of life ($R^2=0.57$, $p<0.01$, $n=20$). Based on their AIC scores, this model was a significant improvement over the model using just the fourth-year temperatures. In the main text, we propose that higher mortality in warmer water is due to enhanced predation. Additional details appear in the section below.

We also found significant negative correlations (high mortality in cold years) for age 7 fish, the oldest age class considered (Table 4). The strongest correlation was with summer temperatures ($r=0.64$, $p<0.01$, $n=20$). The connection between warmer waters and higher survival of larger fish is contrary to our other findings. Due to the low abundance of age 7 fish—on average, age 4 fish are 32 times more abundant and have four times the biomass, we do not consider this further in this paper, but it clearly warrants further study.

Gulf of Maine Cod Steady-State Reference Points

The point of the population dynamics model in Eq. 2 is not to give precise estimates of the population reference points. The model is simpler than the models used in modern stock assessments. For example it uses only a very simple fishing selectivity (age 4 and older are fished at a constant rate). However, the model as designed can capture the relative impact of changes in temperature. The differences in how the three stock-recruit functions represent density dependence have large consequences for the population dynamics. The spawning stock biomass at maximum sustainable yield (SSB_{msy}) for the Ricker function is only weakly dependent on temperature (Fig. 2A). As density dependence weakens, SSB_{msy} increases and becomes more sensitive to temperature. The patterns in the fishing mortality that achieves maximum sustainable yield (F_{msy}) mirror those in SSB_{msy} (Fig. 2B). The function with the strongest density dependence, the Ricker function, has the highest F_{msy} values and is most sensitive to temperature, while the power-law function has almost constant F_{msy} at a very low level. The differences are damped to some degree when considering the actual yield, especially for Ricker and Beverton-Holt (Fig. 2C).

Gulf of Maine Cod Simulations

The differences in density dependence between the three stock-recruit functions lead to a more than 8-fold range in the initial value of the unfished population (Fig. 3A). When normalized by their respective initial values, all have comparable variability until the beginning of the recent warming period (Fig. 3B). At that point, the additional temperature sensitivity in the Beverton-Holt and power-law models becomes more apparent as waters continue to warm. The interannual variability in the populations fished at $F_{msy}(T)$ increases when compared to the unfished populations, with the amount of variability increasing in proportion with the density dependence (Fig. 4A and B). This is due to the increased sensitivity of F_{msy} to temperature.

The three stock-recruit models are difficult to separate statistically, but they paint very different pictures about cod population dynamics. We elected to use the Beverton-Holt model for the main analysis in the paper. It is more widely-used than the power-law model and provides a view of unfished biomass that is more consistent with the high pre-industrial biomass levels (35) than the Ricker model.

We used a simple age-structured model that incorporated temperature-dependent recruitment and age-4 mortality to develop an estimate of SSB_{msy} that accounts for temperature. Our estimated SSB_{msy} declined 33% between 2000 and 2006 and then remained relatively stable over the observation period (Fig. 3, blue). It has been consistently below the current management target, depicted by a population held at the long-term average temperature. We then projected how SSB_{msy} may change under three different temperature scenarios informed by recent climate model projections (34) (Fig. S4). All three scenarios begin with an initial reduction to more normal temperatures followed by warming. The “cool” scenario has the Gulf of Maine temperature anomaly declining to 0.32° and then increasing at a rate of $0.02^\circ \text{ yr}^{-1}$. The “warm” scenario has the Gulf of Maine cooling slightly to 0.5° and then warming at the mean rate from the climate projections of $0.03^\circ \text{ yr}^{-1}$. The “hot” scenario follows the $0.07^\circ\text{C yr}^{-1}$ trend present in the summer temperature time series. Under all three projections, the population declines steadily through 2019 as fish from the recent low recruitment period mature (Fig. 3). The cool and warm scenarios both increase gradually until 2025, while the hot scenario continues to decline. The trends in SSB_{msy} mirror the projected decline in the carrying capacity of the stock (Fig. 3, green).

Influence of Phenology on Mortality

Our analysis found elevated natural mortality in age-4 cod in warmer conditions. We hypothesize that this relationship is due to the phenological changes during warmer years. We expect that mortality in cod is highly seasonal, with more migratory predators present during the warm part of the year. Imagine that there are two seasons: low predation in winter (mortality = m_0), high predation in summer ($x m_0$), where $x > 1$. Assume that the summer season starts at $0.5-d$ and ends at $0.5+d$. The abundance after one year (NI) depends on the initial abundance ($N0$):

$$\begin{aligned} NI &= N0 \exp(-m_0 (0.5-d)) \exp(-x m_0 2 d) \exp(-m_0 (0.5-d)) \\ &= N0 \exp(-m_0 (1+2 d (x-1))) \end{aligned} \quad (\text{Eq. 8})$$

Now, imagine that the high predation season is expanded by $2D$. The new NI is then:

$$NI = N0 \exp(-m_0 (1+2 (d+D) (x-1))) \quad (\text{Eq. 9})$$

We want to know how the change in the seasonality translates into a change in the summer mortality. To do this, we replace x in (Eq. 8) with y , set this equation equal to (Eq. 9), and solve for y :

$$\begin{aligned} N0 \exp(-m_0 (1+2 d (y-1))) &= N0 \exp(-m_0 (1+2 (d+D) (x-1))) \\ -m_0 (1+2 d (y-1)) &= -m_0 (1+2 (d+D) (x-1)) \\ d (y-1) &= (d+D) (x-1) \\ y-1 &= (x-1)(1+D/d) \end{aligned} \quad (\text{Eq. 10})$$

Thus, adding $2D$ to the summer season is equivalent to raising the base rate by $(1+D/d)$. Suppose the high predation season is 3 months ($d=1.5/12 = 0.125 \text{ yr}$). In 2012, the phenology of the Gulf of Maine was accelerated by 20 days in the spring and delayed by a similar amount in the fall. This is equivalent to $D=20/365=0.0548 \text{ yr}$, and $D/d=0.44$. Thus, in 2012, the mortality

rate for cod could have increased by 44% just due to the shift in phenology and without any increase in predator abundance.

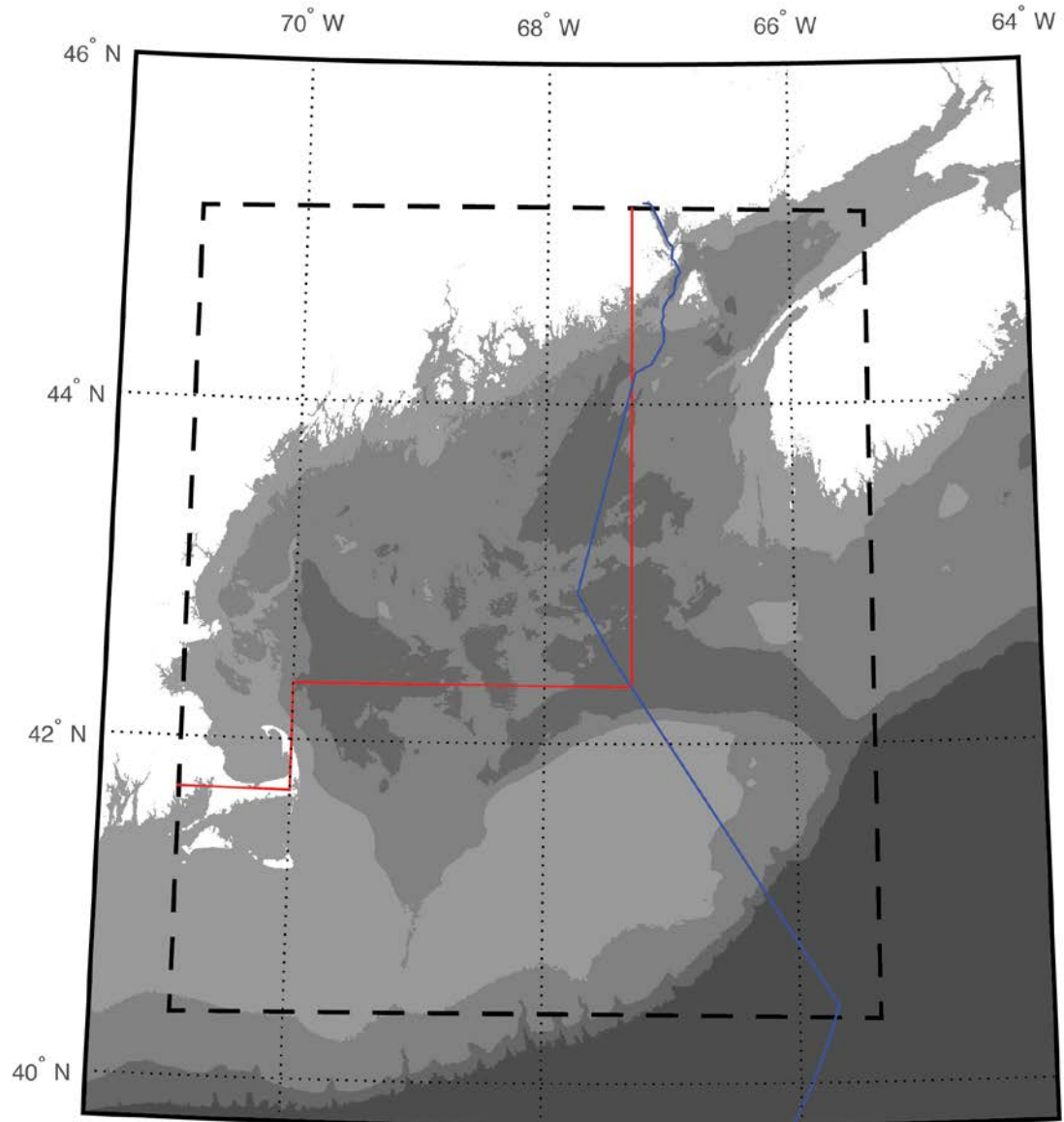


Fig. S1.

Map of the Gulf of Maine. The sea surface temperature time series in Figure 1A is the average temperature anomaly of the region in the dashed line. The temperature time series used in the analysis of Gulf of Maine cod recruitment was averaged over the region outlined by the red line. This is roughly the stock boundary, with the exception of the region east of the Hague Line (blue line) that separates US from Canadian waters.

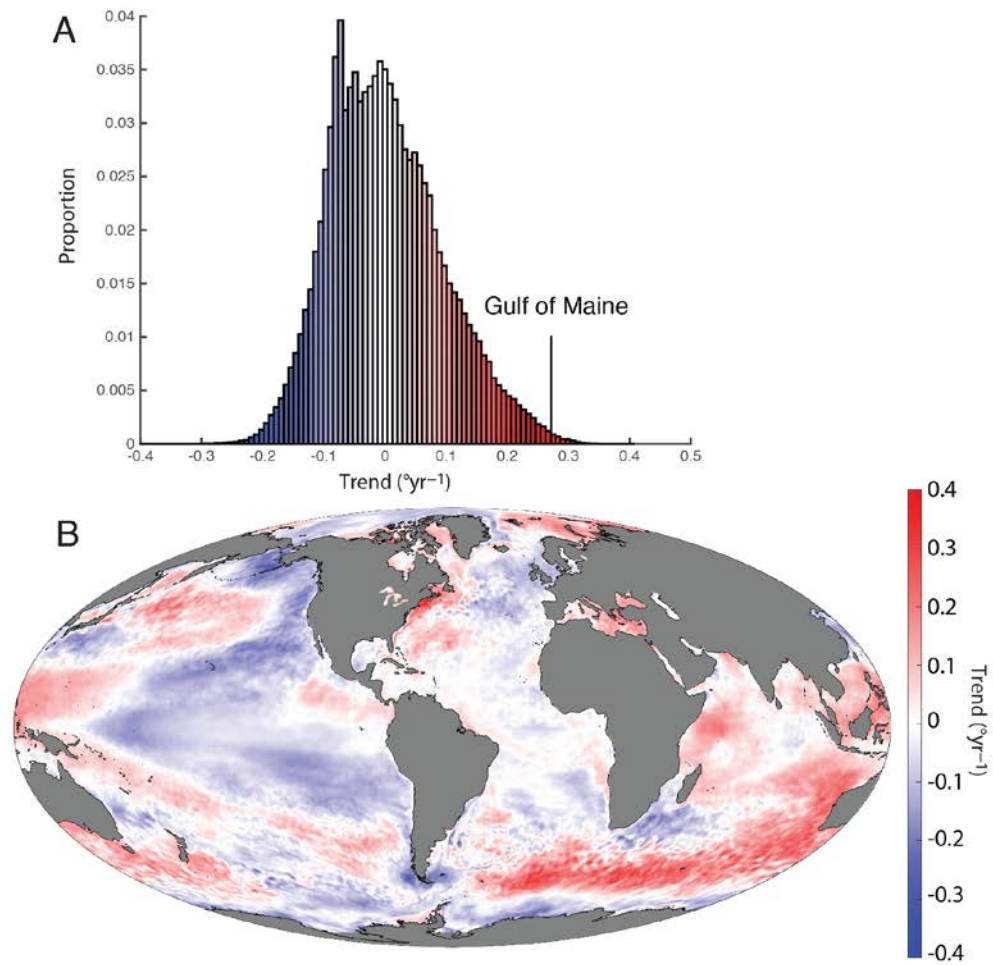


Fig. S2

AVHRR temperature trends scaled by the variance. A. Histogram of trends over 2004-2013. B. Map of 2004-2013 trends. Note: the color scale is different than Figure 1 in the main text.

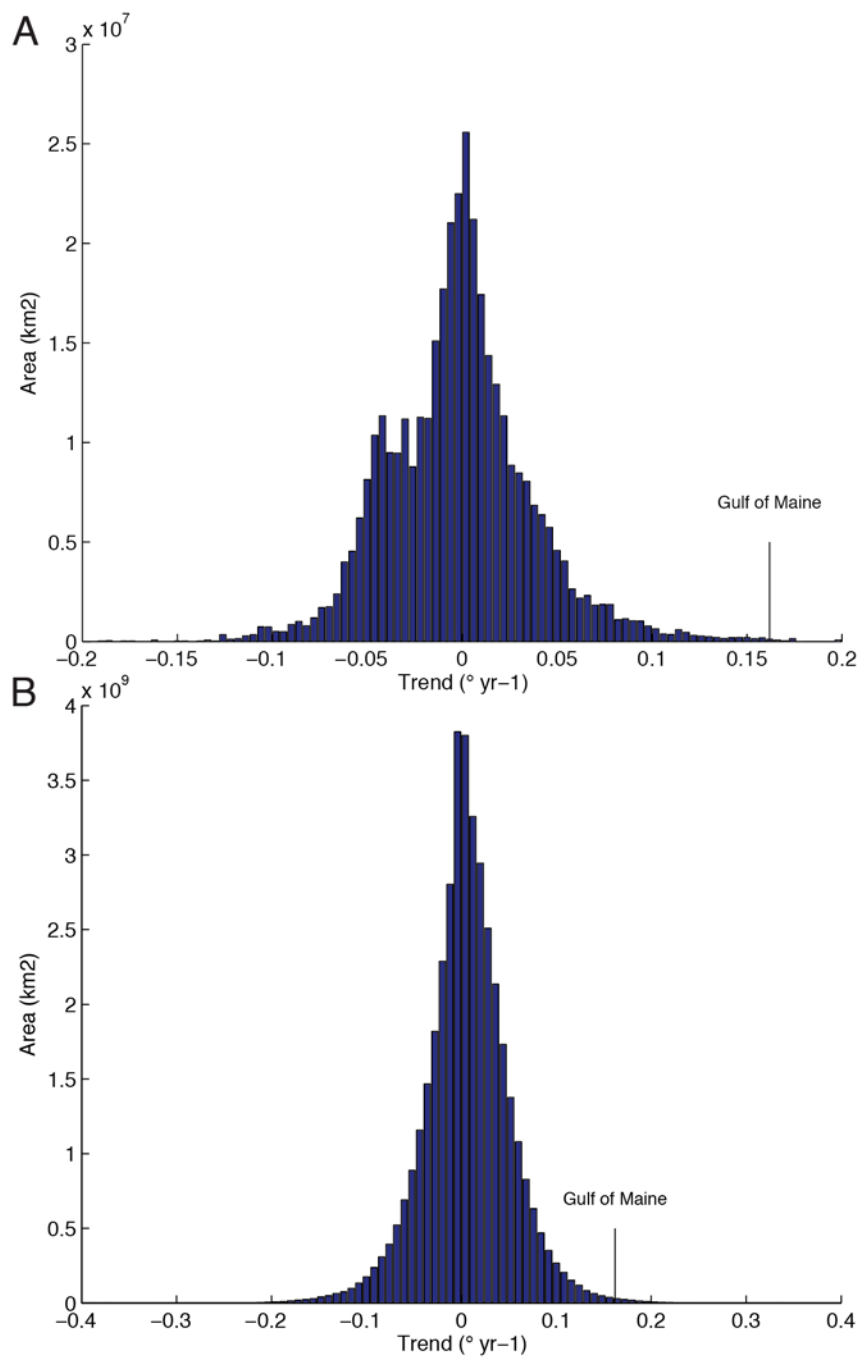


Fig. S3

Area-weighted temperature trends from ERSST. A. Histogram of trends over 2004-2013. B. Histogram of 10 year warming trends from 1900-2013.

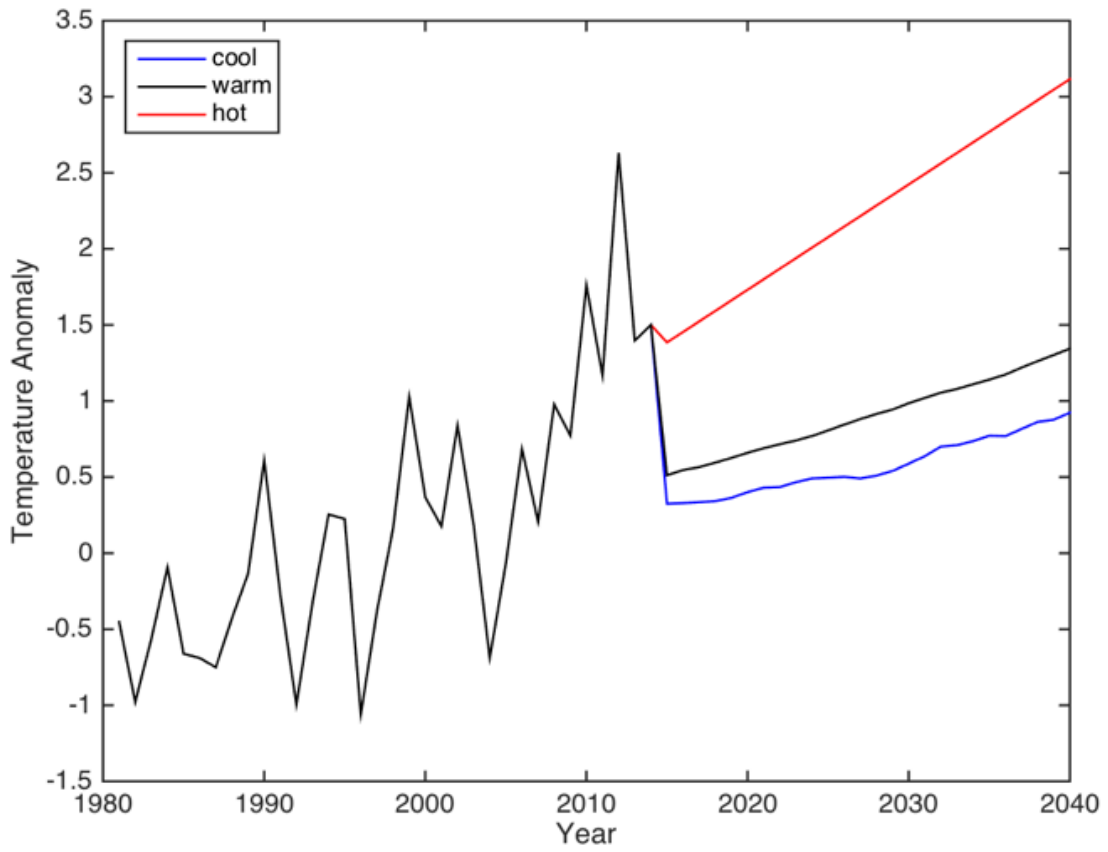


Fig. S4.
Temperature scenarios for the cod population projection.

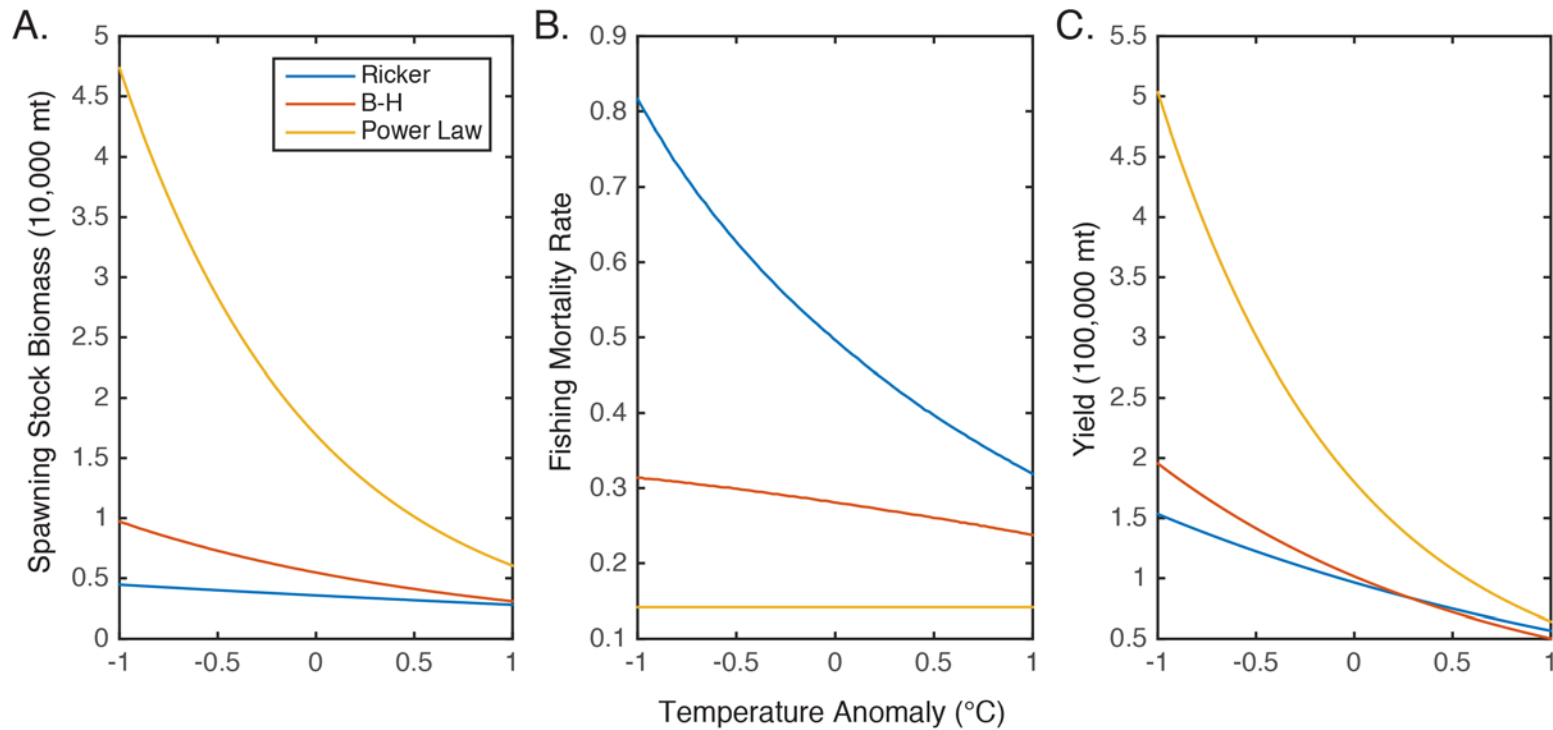


Fig. S5.

Temperature-dependent fishery reference points. Reference points were constructed using the three summer temperature models from Table 1. A. Spawning stock biomass at maximum sustainable yield. B. Fishing mortality rate that achieves maximum sustainable yield. C. Maximum sustainable yield.

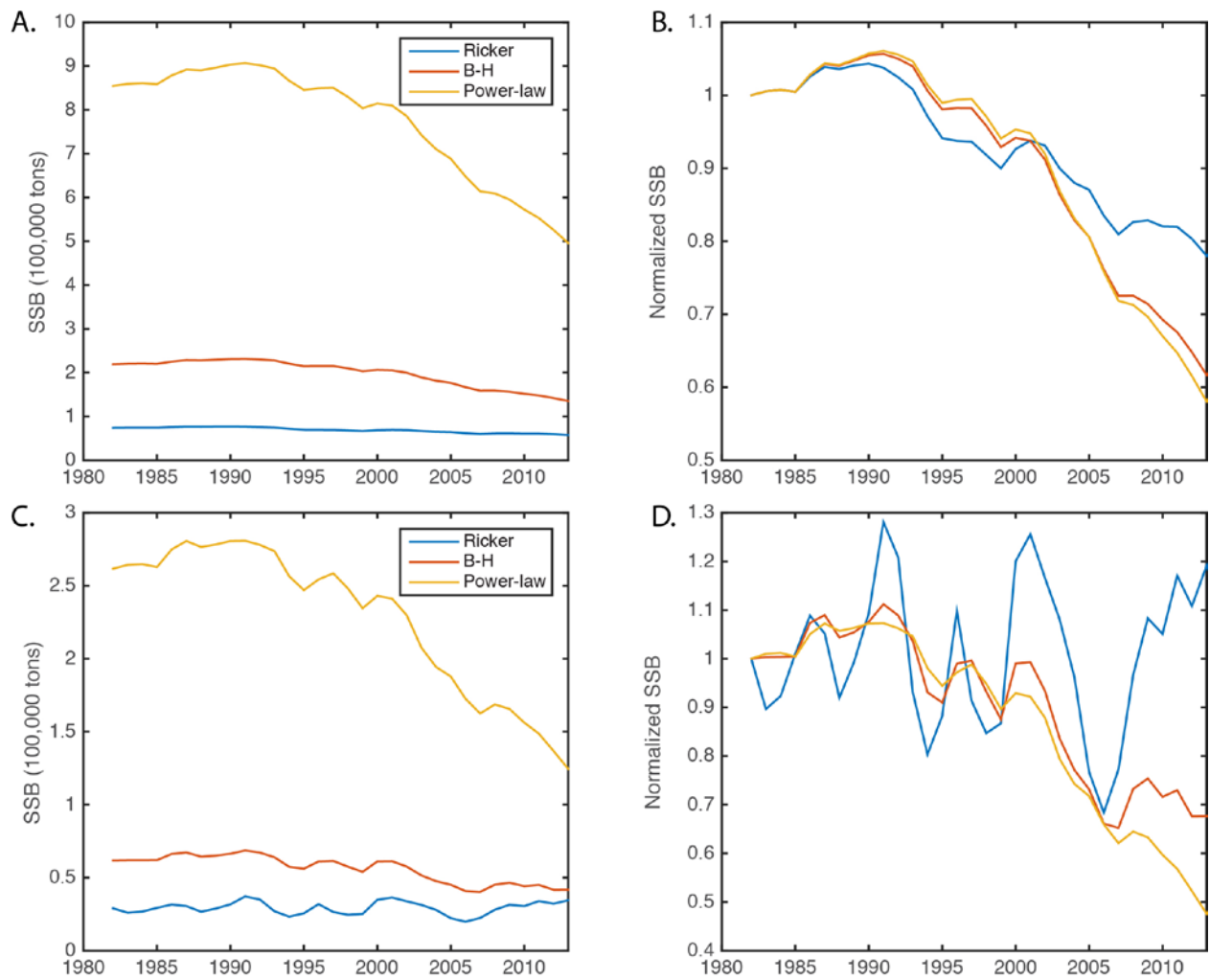


Fig. S6.

Simulated populations using three temperature-dependent stock-recruit functions. Each model was run using observed Gulf of Maine temperatures through 2013. A. SSB (tons) for an unfished population. B. Unfished biomass normalized by the value in the first year. C. SSB (tons) for a population fished at $F_{msy}(T)$, D. fished population biomass normalized by the value in the first year.

Table S1.

Quarterly correlations between Gulf of Maine sea surface temperature and four climate indicators. GSI=Gulf Stream Index, PDO=Pacific Decadal Oscillation, AMO=Atlantic Multidecadal Oscillation, NAO=North Atlantic Oscillation. Correlations were computed over the period 1982-2012, before (“raw”) and after removing linear trends (“detrended”). Correlations significant at the 95% level are highlighted.

Index	Quarter	Raw		Detrended	
		r	p	r	p
GSI	1	0.39	0.03	0.38	0.03
	2	0.52	0.00	0.50	0.00
	3	0.63	0.00	0.64	0.00
	4	0.54	0.00	0.52	0.00
PDO	1	-0.23	0.22	-0.20	0.29
	2	-0.50	0.00	-0.42	0.02
	3	-0.67	0.00	-0.50	0.00
	4	-0.33	0.07	-0.14	0.47
AMO	1	0.03	0.87	-0.07	0.71
	2	0.21	0.26	0.01	0.96
	3	0.48	0.01	0.13	0.50
	4	0.23	0.21	-0.22	0.23
NAO	1	0.09	0.64	0.12	0.51
	2	-0.16	0.40	-0.09	0.64
	3	-0.33	0.07	-0.07	0.69
	4	-0.09	0.65	0.08	0.69

Table S2.

Regression models of cod stock-recruit models. Each of the three stock-recruit models was fit without temperature and then with the quarterly or annual averages for the temperature in the Gulf of Maine stock area. The three best models based on AIC score are highlighted. The out-of-sample performance of each model for the 2004-2013 period are summarized in the last two columns.

Model	1982-2013 Fit			2004-2013 Out of Sample	
	R ²	p	AIC	r ²	p
Ricker	0.29	0.00	28.68	0.23	0.16
Ricker + Q1 SST	0.32	0.00	29.95	0.28	0.12
Ricker + Q2 SST	0.42	0.00	27.67	0.53	0.02
Ricker + Q3 SST	0.55	0.00	23.81	0.59	0.01
Ricker + Q4 SST	0.40	0.00	28.14	0.33	0.08
Ricker + annual SST	0.46	0.00	26.49	0.50	0.02
Beverton-Holt	0.29	0.00	28.68	0.23	0.16
Beverton-Holt + Q1 SST	0.32	0.00	29.95	0.28	0.12
Beverton-Holt + Q2 SST	0.42	0.00	27.66	0.53	0.02
Beverton-Holt + Q3 SST	0.56	0.00	23.42	0.60	0.01
Beverton-Holt + Q4 SST	0.40	0.00	28.14	0.33	0.08
Beverton-Holt + annual SST	0.46	0.00	26.46	0.50	0.02
Power-law	0.29	0.00	28.65	0.22	0.18
Power-law + Q1 SST	0.32	0.00	29.95	0.27	0.12
Power-law + Q2 SST	0.42	0.00	27.57	0.54	0.02
Power-law + Q3 SST	0.57	0.00	23.04	0.61	0.01
Power-law + Q4 SST	0.40	0.00	28.08	0.34	0.08
Power-law + annual SST	0.47	0.00	26.21	0.50	0.02

Table S3.

Regression model coefficients for cod recruitment using summer temperatures. The coefficients for the three models highlighted in Table S2 are shown.

Model	a	b	c
Ricker: $R(S,T)=aS e^{bS+cT}$	0.76	-4.09×10^{-5}	-0.54
Beverton-Holt: $R(S,T)=aS(1+bS)^{-1} e^{cT}$	1.29	1.58×10^{-4}	-0.59
Power-law: $R(S,T)=aS^b e^{cT}$	110.11	4.13×10^{-1}	-0.60

Table S4.

Correlation between the extra mortality needed to correct each age class and the quarterly and annual temperatures in the cod stock region. For each period, correlations were computed with and without the two most recent years. Correlations significant at the 95% level are highlighted.

		1993-2013		1993-2010	
		r	p	r	p
Age 1-2	Q1	0.31	0.19	0.21	0.40
	Q2	0.46	0.04	0.41	0.10
	Q3	0.31	0.18	0.21	0.40
	Q4	0.18	0.45	0.00	0.99
	All	0.36	0.12	0.28	0.26
Age 2-3	Q1	-0.16	0.49	-0.19	0.45
	Q2	-0.10	0.66	-0.11	0.65
	Q3	-0.14	0.57	-0.16	0.52
	Q4	-0.19	0.42	-0.26	0.29
	All	-0.16	0.49	-0.21	0.39
Age 3-4	Q1	-0.03	0.89	0.17	0.51
	Q2	0.00	0.99	0.22	0.37
	Q3	0.09	0.71	0.35	0.15
	Q4	0.27	0.25	0.62	0.01
	All	0.09	0.71	0.40	0.10
Age 4-5	Q1	0.50	0.02	0.37	0.13
	Q2	0.48	0.03	0.35	0.16
	Q3	0.63	0.00	0.53	0.02
	Q4	0.68	0.00	0.50	0.04
	All	0.64	0.00	0.53	0.02
Age 5-6	Q1	0.00	1.00	-0.10	0.70
	Q2	-0.17	0.47	-0.32	0.20
	Q3	-0.11	0.65	-0.25	0.31
	Q4	-0.23	0.33	-0.43	0.07
	All	-0.14	0.54	-0.33	0.18
Age 6-7	Q1	-0.29	0.22	-0.17	0.50
	Q2	-0.21	0.38	-0.06	0.80
	Q3	-0.51	0.02	-0.46	0.05
	Q4	-0.42	0.07	-0.18	0.47
	All	-0.40	0.08	-0.27	0.28
Age 7-8	Q1	-0.35	0.13	-0.13	0.59
	Q2	-0.46	0.04	-0.29	0.24
	Q3	-0.60	0.00	-0.53	0.02
	Q4	-0.51	0.02	-0.50	0.03
	All	-0.55	0.01	-0.44	0.07

Table S5.

Multiple-regression models expressing the extra age-4 mortality from the M=0.2 scenario as a function of one or two temperatures. Models that are significant at the 95% level are highlighted in bold. The top panels are for the period 1993-2012, the bottom are for the period 1993-2010. The Δ AIC values are given relative to the AIC for the best model for each time period. In both cases, this was the model using temperature from the current year and three years before.

Lag	-4			-3			-2			-1			0		
	R ²	p	Δ AIC	R ²	p	Δ AIC	R ²	p	Δ AIC	R ²	p	Δ AIC	R ²	p	Δ AIC
0	1993-2012												0.47	0.00	2.33
-1										0.22	0.04	10.07	0.48	0.00	3.97
-2							0.11	0.15	12.52	0.25	0.09	11.26	0.50	0.00	2.97
-3				0.21	0.04	10.18	0.26	0.08	10.95	0.39	0.01	6.91	0.57	0.00	0.00
-4	0.03	0.49	14.37	0.21	0.13	12.09	0.14	0.28	13.88	0.22	0.12	11.93	0.47	0.00	4.33
0	1993-2010												0.25	0.04	2.23
-1										0.07	0.28	6.00	0.27	0.10	3.75
-2							0.03	0.46	6.74	0.09	0.50	7.69	0.29	0.07	3.13
-3				0.16	0.10	4.14	0.17	0.24	5.91	0.26	0.11	4.01	0.41	0.02	0.00
-4	0.02	0.57	7.00	0.17	0.25	6.07	0.06	0.64	8.29	0.08	0.52	7.78	0.25	0.12	4.20

References

1. E. J. Nelson, P. Kareiva, M. Ruckelshaus, K. Arkema, G. Geller, E. Girvetz, D. Goodrich, V. Matzek, M. Pinsky, W. Reid, M. Saunders, D. Semmens, H. Tallis, Climate change's impact on key ecosystem services and the human well-being they support in the US. *Front. Ecol. Environ.* **11**, 483–493 (2013). [doi:10.1890/120312](https://doi.org/10.1890/120312)
2. R. Mahon, P. McConney, R. N. Roy, Governing fisheries as complex adaptive systems. *Mar. Policy* **32**, 104–112 (2008). [doi:10.1016/j.marpol.2007.04.011](https://doi.org/10.1016/j.marpol.2007.04.011)
3. C. S. Holling, Understanding the complexity of economic, ecological, and social systems. *Ecosystems* **4**, 390–405 (2001). [doi:10.1007/s10021-001-0101-5](https://doi.org/10.1007/s10021-001-0101-5)
4. K. E. Mills, A. Pershing, C. Brown, Y. Chen, F.-S. Chiang, D. Holland, S. Lehuta, J. Nye, J. Sun, A. Thomas, R. Wahle, Fisheries management in a changing climate: Lessons from the 2012 ocean heat wave. *Oceanography* **26**, 191–195 (2013). [doi:10.5670/oceanog.2013.27](https://doi.org/10.5670/oceanog.2013.27)
5. M. C. Palmer, *2014 Assessment Update Report of the Gulf of Maine Atlantic Cod Stock* (U.S. Department of Commerce, 2014).
6. J. A. Nye, J. S. Link, J. A. Hare, W. J. Overholtz, Changing spatial distribution of fish stocks in relation to climate and population size on the Northeast United States continental shelf. *Mar. Ecol. Prog. Ser.* **393**, 111–129 (2009). [doi:10.3354/meps08220](https://doi.org/10.3354/meps08220)
7. J. A. Nye, T. M. Joyce, Y.-O. Kwon, J. S. Link, Silver hake tracks changes in Northwest Atlantic circulation. *Nat. Commun.* **2**, 412 (2011). [Medline doi:10.1038/ncomms1420](https://doi.org/10.1038/ncomms1420)
8. M. L. Pinsky, B. Worm, M. J. Fogarty, J. L. Sarmiento, S. A. Levin, Marine taxa track local climate velocities. *Science* **341**, 1239–1242 (2013). [Medline](https://doi.org/10.1126/science.1239122)
9. T. J. Joyce, C. Deser, M. A. Spall, The relation between decadal variability of Subtropical Mode Water and the North Atlantic Oscillation. *J. Clim.* **13**, 2550–2569 (2000). [doi:10.1175/1520-0442\(2000\)013<2550:TRBDVO>2.0.CO;2](https://doi.org/10.1175/1520-0442(2000)013<2550:TRBDVO>2.0.CO;2)
10. N. J. Mantua, S. R. Hare, The Pacific Decadal Oscillation. *J. Oceanogr.* **58**, 35–44 (2002). [doi:10.1023/A:1015820616384](https://doi.org/10.1023/A:1015820616384)

11. R. A. Kerr, A North Atlantic climate pacemaker for the centuries. *Science* **288**, 1984–1985 (2000). [Medline doi:10.1126/science.288.5473.1984](https://doi.org/10.1126/science.288.5473.1984)
12. L. Wu, W. Cai, L. Zhang, H. Nakamura, A. Timmermann, T. Joyce, M. J. McPhaden, M. Alexander, B. Qiu, M. Visbeck, P. Chang, B. Giese, Enhanced warming over the global subtropical western boundary currents. *Nat. Clim. Change* **2**, 161–166 (2012). [doi:10.1038/nclimate1353](https://doi.org/10.1038/nclimate1353)
13. D. G. Mountain, J. Kane, Major changes in the Georges Bank ecosystem, 1980s to the 1990s. *Mar. Ecol. Prog. Ser.* **398**, 81–91 (2010). [doi:10.3354/meps08323](https://doi.org/10.3354/meps08323)
14. G. G. Gawarkiewicz, R. E. Todd, A. J. Plueddemann, M. Andres, J. P. Manning. Direct interaction between the Gulf Stream and the shelfbreak south of New England. *Sci. Rep.* **2**, 553 (2012). [doi:10.1038/srep00553](https://doi.org/10.1038/srep00553)
15. T. Rossby, R. L. Benway, Slow variations in mean path of the Gulf Stream east of Cape Hatteras. *Geophys. Res. Lett.* **27**, 117–120 (2000). [doi:10.1029/1999GL002356](https://doi.org/10.1029/1999GL002356)
16. A. J. Pershing, C. H. Greene, C. Hannah, D. Sameoto, E. Head, D. G. Mountain, J. W. Jossie, M. C. Benfield, P. C. Reid, T. G. Durbin, Oceanographic responses to climate in the Northwest Atlantic. *Oceanography* **14**, 76–82 (2001). [doi:10.5670/oceanog.2001.25](https://doi.org/10.5670/oceanog.2001.25)
17. K. Chen, G. G. Gawarkiewicz, S. J. Lentz, J. M. Bane, Diagnosing the warming of the Northeastern U.S. Coastal Ocean in 2012: A linkage between the atmospheric jet stream variability and ocean response. *J. Geophys. Res.* **119**, 218–227 (2014). [doi:10.1002/2013JC009393](https://doi.org/10.1002/2013JC009393)
18. B. Planque, T. Frédou, Temperature and the recruitment of Atlantic cod (*Gadus morhua*). *Can. J. Fish. Aquat. Sci.* **56**, 2069–2077 (1999). [doi:10.1139/f99-114](https://doi.org/10.1139/f99-114)
19. K. F. Drinkwater, The response of Atlantic cod (*Gadus morhua*) to future climate change. *ICES J. Mar. Sci.* **62**, 1327–1337 (2005). [doi:10.1016/j.icesjms.2005.05.015](https://doi.org/10.1016/j.icesjms.2005.05.015)
20. M. Fogarty, L. Incze, K. Hayhoe, D. Mountain, J. Manning, Potential climate change impacts on Atlantic cod (*Gadus morhua*) off the Northeastern United States. *Mitig. Adapt. Strategies Glob. Change* **13**, 453–466 (2008). [doi:10.1007/s11027-007-9131-4](https://doi.org/10.1007/s11027-007-9131-4)

21. K. D. Friedland, J. Kane, J. A. Hare, R. G. Lough, P. S. Fratantoni, M. J. Fogarty, J. A. Nye, Thermal habitat constraints on zooplankton species associated with Atlantic cod (*Gadus morhua*) on the US Northeast Continental Shelf. *Prog. Oceanogr.* **116**, 1–13 (2013).
[doi:10.1016/j.pocean.2013.05.011](https://doi.org/10.1016/j.pocean.2013.05.011)
22. J. E. Linehan, R. S. Gregory, D. C. Schneider, Predation risk of age-0 cod (*Gadus*) relative to depth and substrate in coastal waters. *J. Exp. Biol. Ecol.* **263**, 25–44 (2001).
[doi:10.1016/S0022-0981\(01\)00287-8](https://doi.org/10.1016/S0022-0981(01)00287-8)
23. G. D. Sherwood, R. M. Rideout, S. B. Fudge, G. A. Rose, Influence of diet on growth, condition and reproductive capacity in Newfoundland and Labrador cod (*Gadus morhua*): Insights from stable carbon isotopes ($\delta^{13}\text{C}$). *Deep Sea Res. II* **54**, 2794–2809 (2007). [doi:10.1016/j.dsr2.2007.08.007](https://doi.org/10.1016/j.dsr2.2007.08.007)
24. C. Deutsch, A. Ferrel, B. Seibel, H.-O. Pörtner, R. B. Huey, Climate change tightens a metabolic constraint on marine habitats. *Science* **348**, 1132–1135 (2015). [Medline](https://pubmed.ncbi.nlm.nih.gov/26111605/)
[doi:10.1126/science.aaa1605](https://doi.org/10.1126/science.aaa1605)
25. Northeast Fisheries Science Center, *55th Northeast Regional Stock Assessment Workshop (55th SAW) Assessment Report* (U.S. Department of Commerce, 2013).
26. J. D. Dutil, Y. Lambert, Natural mortality from poor condition in Atlantic cod (*Gadus morhua*). *Can. J. Fish. Aquat. Sci.* **57**, 826–836 (2000). [doi:10.1139/f00-023](https://doi.org/10.1139/f00-023)
27. R. W. Reynolds, T. M. Smith, C. Liu, D. B. Chelton, K. S. Casey, M. G. Schlax, Daily high-resolution-blended analyses for sea surface temperature. *J. Clim.* **20**, 5473–5496 (2007).
[doi:10.1175/2007JCLI1824.1](https://doi.org/10.1175/2007JCLI1824.1)
28. B. J. Pyper, R. M. Peterman, Comparison of methods to account for autocorrelation in correlation analyses of fish data. *Can. J. Fish. Aquat. Sci.* **55**, 2127–2140 (1998).
[doi:10.1139/f98-104](https://doi.org/10.1139/f98-104)
29. J. W. Hurrell, Decadal trends in the North Atlantic Oscillation: Regional temperatures and precipitation. *Science* **269**, 676–679 (1995). [Medline](https://pubmed.ncbi.nlm.nih.gov/101126269/) [doi:10.1126/science.269.5224.676](https://doi.org/10.1126/science.269.5224.676)
30. E. P. Ames, Atlantic cod stock structure in the Gulf of Maine. *Fisheries* **29**, 10–28 (2004).
[doi:10.1577/1548-8446\(2004\)29\[10:ACSSIT\]2.0.CO;2](https://doi.org/10.1577/1548-8446(2004)29[10:ACSSIT]2.0.CO;2)

31. A. I. Kovach, T. S. Breton, D. L. Berlinsky, L. Maceda, I. Wirgin, Fine-scale spatial and temporal genetic structure of Atlantic cod off the Atlantic coast of the USA. *Mar. Ecol. Prog. Ser.* **410**, 177–195 (2010). [doi:10.3354/meps08612](https://doi.org/10.3354/meps08612)
32. L. A. Kerr, S. X. Cadrin, A. I. Kovach, Consequences of a mismatch between biological and management units on our perception of Atlantic cod off New England. *ICES J. Mar. Sci.* **71**, 1366–1381 (2014). [doi:10.1093/icesjms/fsu113](https://doi.org/10.1093/icesjms/fsu113)
33. S. M. L. Tallack, Regional growth estimates of Atlantic cod, *Gadus morhua*: Applications of the maximum likelihood GROTAG model to tagging data in the Gulf of Maine (USA/Canada) region. *Fish. Res.* **99**, 137–150 (2009). [doi:10.1016/j.fishres.2009.05.014](https://doi.org/10.1016/j.fishres.2009.05.014)
34. K. E. Taylor, R. J. Stouffer, G. A. Meehl, An Overview of CMIP5 and the experiment design. *Bull. Am. Meteorol. Soc.* **93**, 485–498 (2012). [doi:10.1175/BAMS-D-11-00094.1](https://doi.org/10.1175/BAMS-D-11-00094.1)
35. K. E. Alexander, W. B. Leavenworth, J. Cournane, A. B. Cooper, S. Claesson, S. Brennan, G. Smith, L. Rains, K. Magness, R. Dunn, T. K. Law, R. Gee, W. Jeffrey Bolster, A. A. Rosenberg, Gulf of Maine cod in 1861: Historical analysis of fishery logbooks, with ecosystem implications. *Fish Fish.* **10**, 428–449 (2009). [doi:10.1111/j.1467-2979.2009.00334.x](https://doi.org/10.1111/j.1467-2979.2009.00334.x)